IET Microwaves, Antennas & Propagation

Research Article

IET Journals
The Institution of Engineering and Technology

Transmitarray antenna based on parallel-plate transmission line with high efficiency and large gain bandwidth

ISSN 1751-8725
Received on 12th March 2019
Revised 8th July 2019
Accepted on 9th July 2019
doi: 10.1049/iet-map.2019.0229
www.ietdl.org

Hossein Eskandari[1], *Hamid Reza Hassani*[1] ✉

[1]*Electrical Engineering Department, Shahed University, Persian Gulf Highway, Tehran, Iran*

✉ *E-mail: hassani@shahed.ac.ir*

Abstract: A dual-polarised transmitarray antenna unit cell based on conventional parallel-plate with low loss and wide bandwidth is proposed. A conventional parallel-plate is developed into two new structures; the first structure consists of two sets of parallel-plates forming a four-wall transmission line, while in the second structure the plates of the first structure are replaced by sets of strips. To ease the fabrication, in both cases, the plates are etched on FR4 substrates. These two structures are evaluated as the unit cell of transmitarray antenna to improve the efficiency and gain bandwidth. There is a basic difference between these two unit cells: the first unit cell increases the phase velocity and the second unit cell reduces the phase velocity while passing through the unit cells. Therefore, the layout of the metal antenna plates designed based on the first unit cell becomes concave-like and the layout of the metal antenna plates designed based on the second unit cell becomes convex-like. The antenna designed based on the second unit cell results in higher efficiency as such this antenna is fabricated and measured. The measured results show that the antenna has a peak efficiency of 85.6% and 1 dB gain bandwidth of 22.6%.

1 Introduction

Transmitarray antenna has been a topic of interest for many researchers studying in the field of antenna arrays and great efforts have been made to improve the function of these types of antennas. Transmitarray antennas are widely used in wireless communication, remote sensing of the earth, spatial power combining for high-power applications, and THz imaging and sensors.

There are different approaches to the design of transmitarray antenna and the most important ones include three approaches of multi-layer frequency selective surfaces (M-FSS), receiver–transmitter design and metamaterial/transformation approach [1].

In the first approach, the FSS structure is used for phase compensation, but since the single layer alone cannot compensate for the 360° phase range, the multilayered FSS is employed [2, 3]. The use of multilayered dielectric substrate increases the losses and thus, reduces the efficiency. If the substrate is removed in these structures [4–7], although efficiency is improved, the structure of the antenna becomes very fragile, which is not appropriate to be used in equipment with vibration and tension. For instance, letter [7] has reported a 10.3 GHz antenna that has 62% efficiency with 24.7% 1 dB gain bandwidth. In that paper, five brittle metal layers with no dielectric substrate have been used.

In the second approach, two layers of printed antenna arrays are placed on top of each other, each element of one layer is coupled to that of the other layer via a transmission line or aperture coupled patch. The transmission line or aperture coupled patch is used to provide the required phase delays for the transmitarray antenna [8, 9].

In the third approach, the required phase shift for each element of the array is obtained through changes in the effective substrate permittivity and permeability using metamaterial configuration [10, 11].

In addition to the commonly used approaches, the use of perforated 3D all-dielectric is another approach of transmitarray antenna design [12–16]. In this approach, the entire transmitarray antenna is a piece of thick dielectric and does not contain metal and the transmission phase through the dielectric can be controlled through changing the size of the holes within the dielectric.

In the previous works, either efficiency or gain bandwidth has been improved; they have not been improved at the same time.

In this paper, a transmitarray antenna based on a new approach in which both the efficiency and gain-bandwidth characteristics are improved simultaneously is proposed. The novelty of this approach is the use of the slow-wave structure [17] based on the parallel plate to improve transmitarray antenna gain bandwidth and efficiency at the same time. In the proposed approach, unit cells are introduced based on the parallel plate transmission line, the length of which controls the amount of required phase shift. Based on the type of the parallel plates used, in one type the unit cell increases the velocity of the guided wave (fast wave) thus acting as high-pass filter, while in the other type it reduces the velocity of the guided wave (slow wave) and acts as a low-pass filter. Furthermore, due to the low-pass filter behaviour of the second unit cell, the unit cell has a smaller opening resulting in a larger number of unit cells within the antenna aperture. This results in smoother phase variations between adjacent cells. Therefore, the phase correction is close to the ideal state and increases the antenna efficiency.

2 Unit cell design

The parallel-plate that is used as the main element of the proposed unit cell is used as a transmission line to provide the required phase shift. To have a dual-polarised transmitarray antenna, i.e. with the same performance in both TE1 and TM1 polarisation, a unit cell structure in which two sets of the parallel plate arranged to form a four-wall transmission line, as shown in Fig. 1*a*, is used. It should be noted that the structure of Fig. 1*a* is hollow and the dielectric substrate used in unit cells is only to support the metal plates. If these substrates are removed, we obtain the usual two sets of orthogonal parallel plates.

In order to implement such a structure in practice, the parallel metal plates are printed on a low-cost substrate FR4 with permittivity of 4.4. The substrate is mostly used for ease of fabrication of the transmitarray antenna and its permittivity and loss tangent is not that important. The unit cell is simulated by using the CST software package to obtain the transmission and reflection responses.

The length of the parallel plate L, shown in Fig. 1, can be changed in order to obtain the required phase correction of the aperture surface of the transmitarray antenna.

The unit cell structure with two sets of the parallel plate arranged to form a four-wall transmission line is dual polarised, the

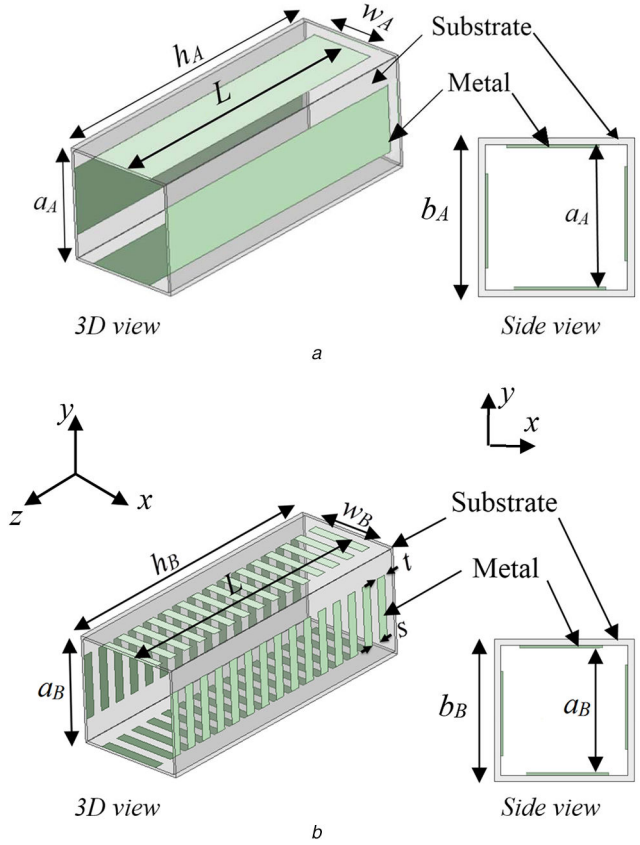

Fig. 1 *3D and left side view of unit cells*
(a) Unit cell *A* with two sets of parallel plates, ***(b)*** Unit cell *B* with stripes

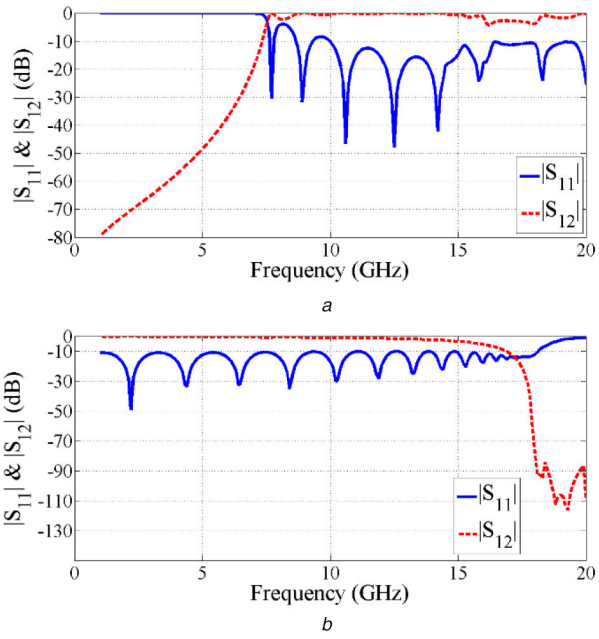

Fig. 2 *Transmission and reflection response versus frequency*
(a) Unit cell *A*, ***(b)*** Unit cell *B*

sense of which is determined by feed polarisation and is called a unit cell *A*.

From Fig. 1*a*, the design parameters are b_A, a_A, w_A, h_A and L. Using these parameters, the unit cell structure can be optimised to design the transmitarray antenna with high efficiency and large 1 dB gain bandwidth. The centre frequency of 11 GHz is selected and the unit cell is simulated in the Floquet mode of CST software package.

The cut-off frequency of the parallel plate waveguide is based on the following equation:

$$f_{cA}(\mathrm{TE1, TM1}) = \frac{1}{2a_A\sqrt{\mu\varepsilon}} = \frac{c}{2a_A} \text{ if } f > f_{cA} \text{ then } a_A > \frac{\lambda_0}{2} \quad (1)$$

where a_A is the distance between the parallel metal plate, c is the speed of light and λ_0 is the wavelength in free space at 11 GHz frequency. According to (1), the dimension of a_A should be, $a_A > \lambda_0/2$.

The distance between parallel-plate is selected to be $0.75\lambda_0$ (a_A = 20.5 mm) to activate TE1 and TM1 mode between the plates. Through optimisation considering the overall size of the structure and the relevant responses, the dimensions of the unit cell *A* are chosen as: b_A = 21 mm ($0.77\lambda_0$), a_A = 20.5 mm ($0.75\lambda_0$), w_A = 20.425 mm ($0.749\lambda_0$) and h_A = 85.5 mm ($3.1\lambda_0$).

The transmission coefficient magnitude (S_{12}) of the unit cell *A* is plotted against frequency in Fig. 2*a*.

According to (1) and Fig. 2*a*, it can be seen that the unit cell *A* is suitable for frequencies higher than 7.3 GHz and acts like a high-pass filter, with a cut-off frequency of 7.3 GHz.

If the phase velocity (2) is considered, it is seen that for frequencies higher than the cut-off frequency, the phase velocity is more than the speed of light. In the other words, if $f > f_c$ then $v_p > c$. Therefore, the unit cell *A* increases the phase velocity and the unit cell *A* is the fast wave structure. To illustrate this, the dispersion curve of the unit cell *A* is obtained from (2) and (3), where β is phase constant. The dispersion diagram is plotted as frequency versus absolute value of β/π, and is shown in Fig. 3. The expression of light line, which separate the fast-wave ($\beta < k_0$) and slow-wave ($\beta > k_0$) regions (where k_0 is the free space wavenumber) is given by (4). According to Fig. 3, the unit cell *A* is located in the fast wave region

$$v_p = \frac{c}{\sqrt{1 - \left(f_c^2/f^2\right)}} \quad (2)$$

$$v_p = \frac{2\pi f}{\beta} \quad (3)$$

$$\text{Light line: } \frac{k_0}{\pi} = \frac{\omega}{\pi c} \rightarrow \frac{k_0}{\pi} = \frac{2}{c} f \quad (4)$$

As shown below, the fast wave unit cell *A* leads to a concave-like lens [18] for the transmitarray antenna aperture layout.

In order to achieve higher gain, it is necessary to have a unit cell that can provide at least 360° of phase shift [1]. The simulated transmission phase shift response diagram based on the length changes of unit cell *A* for various frequencies (f = 10, 11 and 12 GHz) is shown in Fig. 4*a*. These results are obtained based on applying infinite-periodic boundary conditions on four planes, and Floquet ports. As shown in Fig. 4*a*, the phase changes are parallel to each other and properly cover the 360° required.

Equation (5) gives the relationship between ΔL and $\Delta\varphi$ as obtained from Fig. 4*a* for centre frequency of 11 GHz

$$\Delta L = 0.2375\,\Delta\varphi \quad (5)$$

where ΔL is the change in unit cell length and $\Delta\varphi$ is the required phase difference.

In the final transmitarray antenna design, the value of each unit cell length is obtained from Fig. 4*a* (or from (5)) for the required phase.

The amplitude of transmission and reflection responses are shown in Fig. 5*a* to prove that the unit cell *A* in the range of length variations have acceptable values.

In order to increase the antenna aperture efficiency one requires a smoother antenna aperture phase variation (ideal state). This can be obtained by having a smaller opening unit cell.

According to Fig. 2*a* and (1), as the opening of unit cell *A* becomes smaller, the cut-off frequency would move to higher frequencies. Therefore, unit cell *A* would not have a good transmission response at the designed frequency and there would

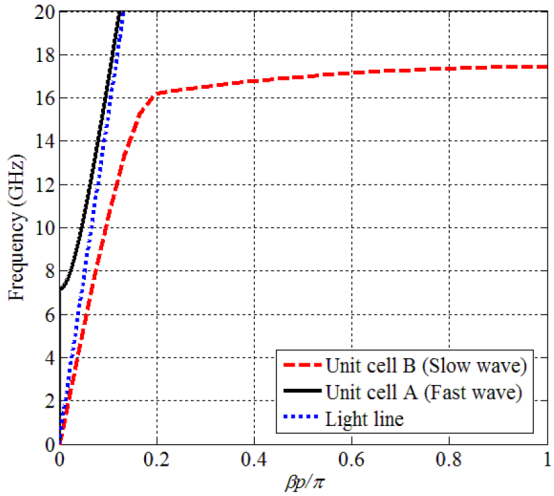

Fig. 3 *Dispersion diagram for the unit cells A and B*

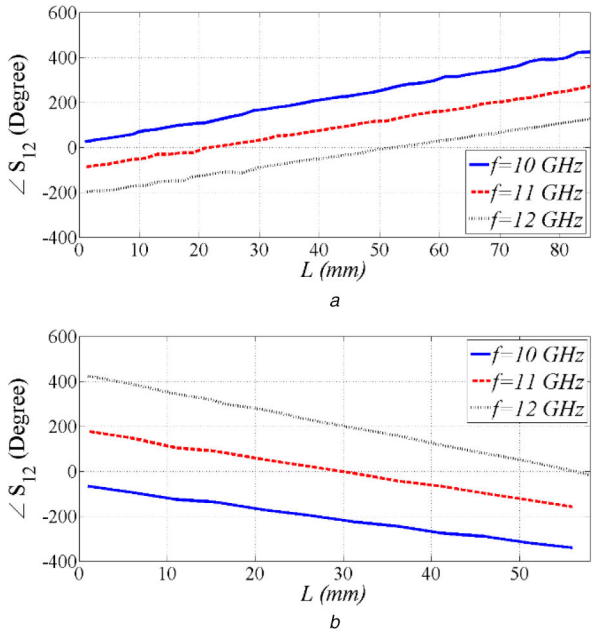

Fig. 4 *Transmission phase shift response against the length of unit cell A for various frequencies*
(a) Unit cell *A*, ***(b)*** Unit cell *B*

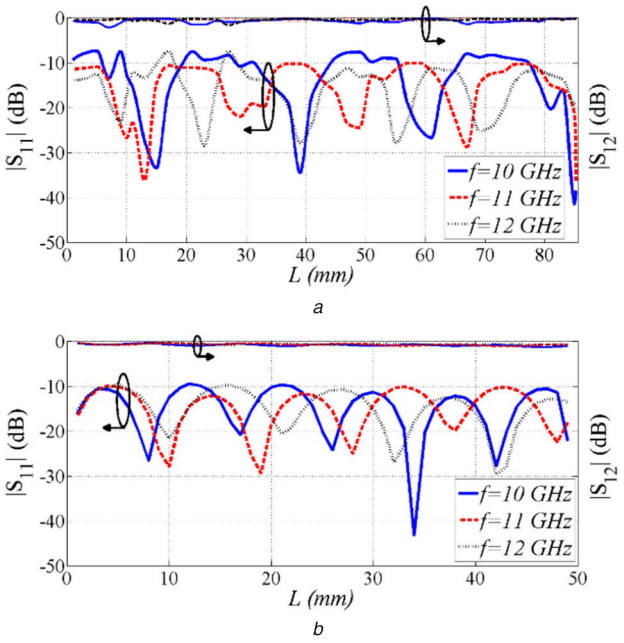

Fig. 5 *Transmission and reflection responses against the length of the unit cell A for various frequencies*
(a) Unit cell *A*, ***(b)*** Unit cell *B*

be a large reflection from the unit cell that would not be appropriate for transmitarray antenna.

In order to simultaneously fulfil the small opening of the unit cell and to have good transmission parameter (S_{12}), the structure of unit cell *B* is introduced, as shown in Fig. 1*b*. As seen in the figure, structure *B* is similar to structure *A*, with the difference that there are metal strips on the walls, instead of a full solid metal surface.

Through optimisation considering the overall size of the structure, the relevant responses, and the complexities of the strips in the fabrication, the dimensions of the unit cell *B* are chosen as: $b_B = 9$ mm ($0.33\lambda_0$), $a_B = 8.5$ mm ($0.31\lambda_0$), $w_B = 5$ mm ($0.18\lambda_0$), $s =$ 1 mm, $t = 0.2$ mm and $h_B = 58$ mm ($2.1\lambda_0$).

The transmission (S_{12}) and reflection (S_{11}) responses of the unit cell *B* are plotted in Fig. 2*b*. It can be seen that the unit cell *B* is suitable for frequencies lower than 17.6 GHz, i.e. unit cell *B* acts as a low-pass filter with cut-off frequency (f_c) given by

$$f_{cB}(\mathrm{TE1,TM1}) = \frac{1}{2a_B\sqrt{\mu\varepsilon}} = \frac{c}{2a_B} \text{if } f < f_{cB} \text{ then } a_B < \frac{\lambda_0}{2} \quad (6)$$

Equation (6) is the same as (1), except that (1) is for high-pass filter and (6) is for low-pass filter. Both equations are derived from the conventional equation of the parallel plate, which confirm the simulation results of cut-off frequency, as shown in Fig. 2*b*.

According to (6), a_B is selected to be $0.31\lambda_0 = 8.5$ mm at 11 GHz frequency. As the opening of unit cell *B* becomes smaller, the cut-off frequency would move to higher frequencies and it would have good transmission response at the designed frequency that would be appropriate for the transmitarray antenna.

Thus, given that the dimensions of the opening of structure *B* are smaller than the dimensions of the opening of structure *A*, structure *B* would cover the effective aperture of the transmitarray antenna with more cells and smooth phase variations. Therefore, the phase distribution on the antenna aperture becomes closer to the ideal state.

The dispersion curve of the unit cell *B* is analysed using commercial EM software CST under the eigenmode analysis, in which one periodic unit cell *B* in *z*-direction ($p = 1.2$ mm) is modelled to obtain the dispersion curve. The dispersion diagram of unit cell *B* is shown in Fig. 3. The light line determines the separation between fast-wave ($\beta < k_0$) and slow-wave ($\beta > k_0$) regions. Thus, the unit cell *B* is located in the slow-wave region. According to Fig. 3, as *f* increases in the range of $0 < f < f_c$, the slopes of unit cell *B* curves decrease and the slow-wave specification appears.

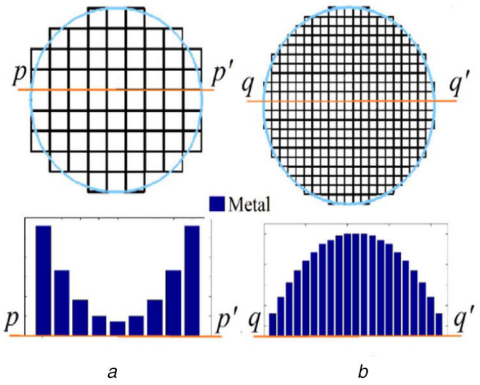

Fig. 6 *Front view of the transmitarray antenna and its cross-sectional view*
(a) Transmitarray *A*, ***(b)*** Transmitarray *B*

The variations of the transmission phase shift response, and the transmission and reflection magnitude response of the unit cell *B* versus length of the unit cell for various frequencies ($f = 10$, 11 and 12 GHz) are shown in Figs. 4*b* and 5*b*, respectively. As shown in Fig. 4*b*, the variation of the phase changes in structure *B* for various frequencies is parallel to each other and they properly cover the range of 360°. For the centre frequency of 11 GHz, the variations are according to the following equation:

$$\Delta L = -0.16\Delta\varphi \tag{7}$$

where ΔL is the change of the unit cell length and $\Delta\varphi$ is the phase change required.

Using the results of Fig. 4*b* or (7), the value of the unit cell length for the given phase is obtained.

According to Fig. 5*b*, the unit cell *B* has a good magnitude transmission response despite the cell small opening.

3 Transmitarray antenna *A* and *B*

Based on the results obtained in the previous section, the unit cells *A* and *B* have large phase range, large bandwidth, low reflection, low insertion loss, and the transmission phase shift response can be easily controlled through varying the unit cell length, therefore, these are used to design the transmitarray antenna.

The transmitarray antenna designed with unit cell *A* is named transmitarray *A*, and the transmitarray designed with unit cell *B* is named transmitarray *B*.

In both cases, the transmitarray antenna is designed in an overall circular shape aperture for operation at the frequency of 11 GHz, $F/D = 1$ and with the diameter of 189 mm = $6.93\lambda_0$ (in which λ_0 is the free space wavelength). A $F/D = 1$ is selected to provide ~10 dB of edge taper in the *E*-plane. For comparison, *F* and *D* are considered the same for both antennas and set at 189 mm. The diameter *D* of transmitarray *A* and *B* is obtained as

$$D_{A\,\text{or}\,B} = N_{A\,\text{or}\,B} \times b_{A\,\text{or}\,B} \tag{8}$$

where *N* is the number of cells along the main diameter of transmitarray *A* and *B*, and *b* is the square side length of the unit cell. Then, the diameter of the transmitarray *A* and *B* would be

$D_A = 9 \times 21$ mm = 189 mm

$D_B = 21 \times 9$ mm = 189 mm

The transmitarray array is fed with a symmetric corrugated X-band horn antenna with the same *E*- and *H*-plane patterns. The horn has 15.5 dBi gain at the frequency of 10 GHz. The pattern of this horn follows the pattern of $\cos^{15}(\theta)$. This horn is the one used in [4–6]. The horn is placed at distance *F* from the centre of the transmitarray.

3.1 Transmitarray antenna A

Based on the unit cell of Fig. 1*a*, and as mentioned before, the opening size of unit cell *A* is selected to be 21 mm × 21 mm (i.e. $0.77\lambda_0 \times 0.77\lambda_0$ at the design frequency 11 GHz). According to Fig. 4*a* and (5), by changing the length of the metal plate printed on the FR4 substrate, the value of phase shift is obtained to compensate for the required phase of the transmitarray antenna aperture surface. If the origin of the coordinates is considered in the middle of the aperture of the transmitarray antenna, the layout of a row of unit cell metal plates would be as shown in Fig. 6*a*. As seen in the figure, with respect to the dimensions of the opening of unit cell *A*, i.e. $b_A = 21$ mm, over the diameter of the transmitarray antenna with the dimension of $D = 189$ mm, only nine unit cells could be used.

In addition, the metal plates of unit cell *A* form a concave shape, which indicates that the unit cell *A* attempts to correct or compensate for the required phase of the aperture surface of the transmitarray antenna by raising the phase velocity of the wave. Fig. 6*a* shows a circle of diameter 189 mm in which 65 of 21 × 21 mm^2 unit cells are arranged.

All structures are simulated by using the CST software package and MATLAB to obtain the phase distribution, gain and pattern.

The compensated phase distribution for one quarter of the aperture, for transmitarray *A* is shown in Fig. 7.

According to Fig. 7*a*, the compensated phase distribution of unit cell *A* is far away from ideal state.

Results of the simulating realised gain and efficiency per frequency are shown in Figs. 8 and 9. The results show that −1 dB gain bandwidth obtained from this antenna is 2.9 GHz (10–12.9 GHz), which is 25.3% of the related centre frequency, and the maximum efficiency is 54.4%. In addition, the value of gain over this bandwidth is more than 23.2 dBi.

The efficiency is calculated using (9), where *G* is the realised gain, and *A* is the area of the transmitarray circular aperture

$$\eta_{\text{aperture}} = \frac{G\lambda_0^2}{4\pi A} \tag{9}$$

3.2 Transmitarray antenna B

As shown in Fig. 1*b*, the opening size of unit cell *B* is set at 9 mm × 9 mm (i.e. $0.33\lambda_0 \times 0.33\lambda_0$ at the design frequency 11 GHz). According to Fig. 4*b* and (7), by changing the number of the strip-metal plates printed on the FR4 substrate, the value of phase shifts to compensate for the required phase of the transmitarray antenna aperture surface is obtained.

If the origin of the coordinates is considered in the middle of the aperture of the transmitarray antenna, the layout of a row of unit cell metal plates would be as shown in Fig. 6*b*. Accordingly, over the diameter of the transmitarray, $D = 189$ mm, considering the dimensions of unit cell *B*, $b_B = 9$ mm, only 21 unit cells can be used. In addition, it is clear unlike the previous antenna *A*, this antenna *B* presents a convex shape.

This shows that the unit cell *B* attempts to compensate for the required phase of the transmitarray aperture surface by causing delays in the electromagnetic wave (reducing phase velocity). In Fig. 6*b*, placement of unit cells *B* over the circle with the diameter of 189 mm is shown.

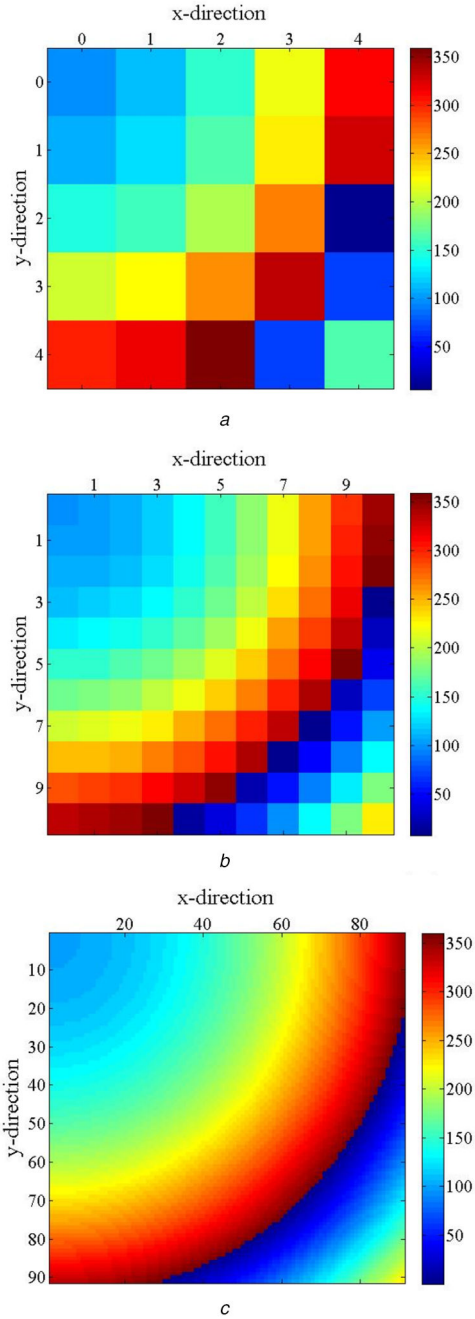

Fig. 7 *Compensated phase distribution for one-quarter of the transmitarray antenna aperture*
(a) Transmitarray *A*, ***(b)*** Transmitarray *B*, ***(c)*** Ideal state

The results of realised gain and aperture efficiency simulations versus frequency for transmitarray *B* are shown in Figs. 8 and 9, respectively. The results show that the −1 dB gain bandwidth obtained from this antenna is 2.7 GHz (9.7–12.4 GHz), i.e. 24.4%, in the centre frequency, and the value of gain over the bandwidth is more than 25 dBi. The maximum simulated efficiency of this antenna is 87.6%.

One can also see that gain of transmitarray *B* is higher than that of transmitarray *A* by around 2.5 dB. As stated before, the aperture surface area of both transmitarray *A* and *B* are kept the same. Both are fed by the same horn feed and have the same F/D ratio. Thus, one assumes that spill over, taper, blockage efficiencies and so on are the same for both cases. The only difference would be the quantisation phase error leading to this difference in antenna gain.

For comparison, the compensated phase distribution for one-quarter of the aperture, for transmitarray *A*, *B* and the ideal state is shown in Fig. 7. It is known that the phase of each transmitarray element is selected to provide the closest quantisation phase with respect to the ideal phase shift [1]. The smaller the size of the unit

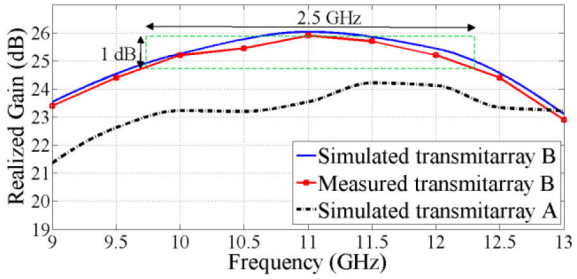

Fig. 8 *Realised gain of transmitarray A and B*

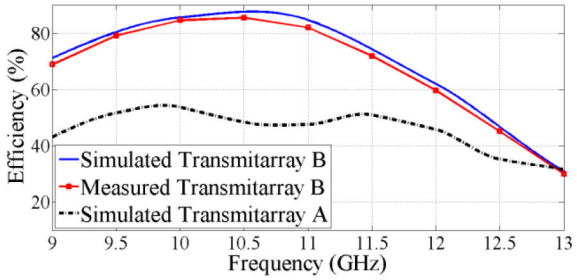

Fig. 9 *Efficiency of transmitarray A and B*

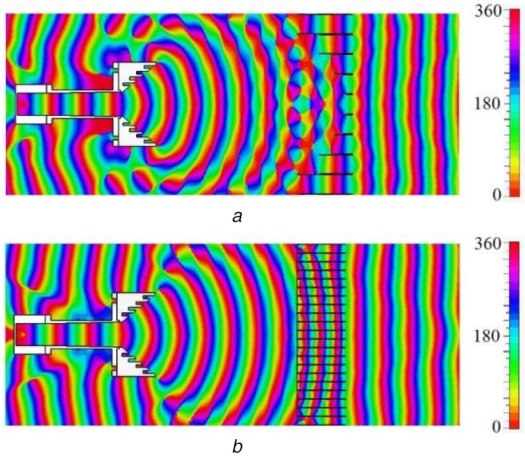

Fig. 10 *Phase of E-field distribution in y–z plane*
(a) Transmitarray *A*, ***(b)*** Transmitarray *B*

cell the closest we can get to the ideal phase shift. Not in every unit cell design one can reduce the cross-section size of the unit cell without affecting the magnitude of S_{11} or S_{12}. However, in the proposed unit cell *B*, as the cross-section of the unit cell becomes smaller, the S_{11} and S_{12} will remain as desired. This is due to the low-pass filter and slow-wave nature of the structure that leads to the operating frequency to be within 0 to f_c. Thus, the size of the unit cell *B* can be reduced and it leads to the decrease of the quantisation phase errors. This effect cannot be obtained through unit cell *A* since it has a high-pass filter behaviour and when the cross-section of unit cell *A* becomes smaller, the cut-off frequency moves upwards and the operating frequency would then be lower than f_c.

According to Fig. 7, since we can reduce the size of the unit cell *B*, the compensated phase distribution would be much closer to that of the ideal case, while unit cell *A* is far away from the ideal state. Thus, antenna *B* would have a lower quantisation error and higher efficiency.

In addition, the phase distribution of the electric field at frequency of 11 GHz for both transmitarray antennas *A* and *B* along the *y*-axis are shown in Fig. 10. These clearly show how the electromagnetic waves become in-phase after passing through the transmitarray *A* and *B*.

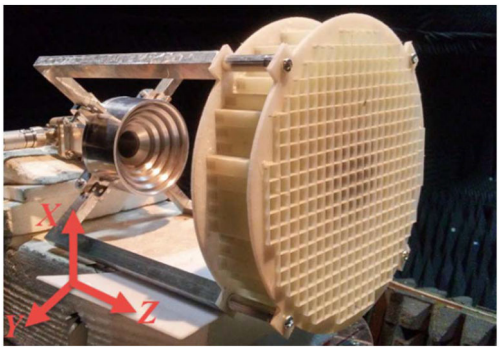

Fig. 11 *Fabricated transmitarray antenna B*

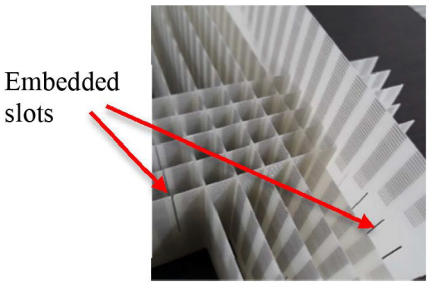

Fig. 12 *Rectangular blades with embedded slots for the assembly of rectangular blades*

Table 1 Comparison of transmitarray antennas *A* and *B*

Parameter	Transmitarray *A*	Transmitarray *B*	
	Simulated	Simulated	Measured
1 dB gain BW	25.3%	24.4%	22.6%
efficiency	54.4%	87.6%	85.6%
N	9	21	
D (mm)	189 ($6.93\lambda_0$)	189 ($6.93\lambda_0$)	
total unit cell	65	341	
unit cell size	$21^2 \times 85.5$ mm^3 $(0.77\lambda_0)^2 \times 3.1\lambda_0$	$9^2 \times 58$ $(0.33\lambda_0)^2 \times 2.1\lambda_0$	
array size	94.52π mm^2 $(3.47\lambda_0)^2\pi$	94.52π $(3.47\lambda_0)^2\pi$	
unit cell type	fast wave	slow wave	

4 Transmitarray antenna *B* measurement

According to the results of the simulations, the transmitarray antenna *B* provides higher efficiency and almost the same 1 dB gain bandwidth compared to the transmitarray antenna *A*. Thus, antenna *B* is fabricated and is shown in Fig. 11.

The structure of transmitarray antenna *B* is made on FR4 substrate with permittivity of 4.4 and has a thickness of 0.5 mm. In all, 21×21 rectangular dielectrics of width 58 mm and different length are used. On each of these dielectrics, strip metals are printed on both sides using PCB technology. Between each row of strips, a slot is placed. As shown in Fig. 12, these rectangular dielectrics are inserted into each other through the slots, forming the structure shown in Fig. 11.

FR4 substrate is chosen in order to reduce the cost of fabrication. It should be noted that this substrate is used to hold the metal plates and change in effective permittivity (ε_r) does not have a considerable effect on the output characteristics of the transmitarray antenna.

The measured and simulated realised gain and efficiency are shown in Figs. 8 and 9, respectively.

From the measured realised gain, the maximum gain of 25.9 dB, maximum efficiency of 85.6% and −1 dB gain bandwidth of 22.6% (9.8–12.3 GHz) are obtained.

For comparison, the specifications of the transmitarray antennas *A* and *B* are listed in Table 1.

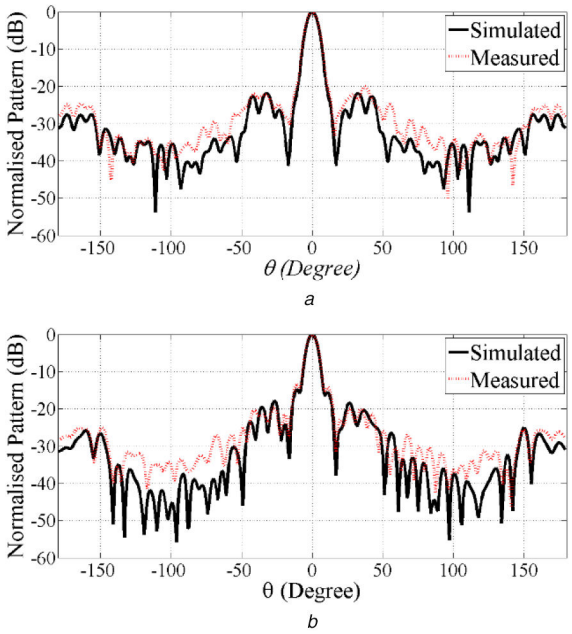

Fig. 13 *Measured and simulated normalised pattern of transmitarray B at frequency 11 GHz*
(a) *x–z* plane, ***(b)*** *y–z* plane

The simulated and measured antenna patterns for the 11 GHz frequency on both *x–z* and *y–z* planes are shown in Fig. 13. The small difference between simulation and measurement results might be due to fabrication and assembling tolerances. As shown in Fig. 13, the fabricated antenna has a side-lobe of −20 dB in the *x–z* plane and −14.5 dB in the *y–z* plane, which is acceptable value.

The main performance and physical dimension of the fabricated transmitarray antenna *B* are presented in Table 2 and compared with the recent transmitarray antennas presented in [14–16], and [19–23].

5 Conclusion

A new dual-polarised transmitarray antenna providing large bandwidth and high efficiency based on printed parallel-plate transmission line has been presented. The novelty of this approach is the use of the slow-wave structure for the design of the transmitarray antenna to improve its performance. The parallel-plate transmission line is developed and two new unit cells are introduced. The structure of the first proposed unit cell consists of two sets of parallel plates forming a four-wall transmission line that increases the phase velocity (fast wave) while the wave passes through the unit cell. The layout of the metal plates of such transmitarray antenna is of concave shape. The second unit cell proposed consists of a set of strips on the four walls of the transmission line in such a way that decreases the phase velocity (slow wave) of the wave when it passes through the unit cell. The layout of this proposed transmitarray antenna is of convex shape. Compared to the concave type transmitarray, the convex type due to having a larger number of unit cells over the antenna aperture

Table 2 Comparison between the proposed antenna *B*, and previous reported

Ref.	Frequency, GHz	Array size, λ_0^2	Unit cell size, λ_0^2	Overall thickness, λ_0	Aperture efficiency, %	1 dB gain BW, %
[14]	94	18.17 × 18.17	0.63 × 0.63	1.31	25	15.9
[15]	60	9.5 × 9.5	0.5 × 0.5	2	20	17
[16]	12.5	$(7.5)^2\pi$	0.25 × 0.25	1.21	54.1	—
[19]	30.25	12.6 × 12.6	0.6 × 0.6	0.96	47	7.5
[20]	13.5	$(7.24)^2\pi$	0.5 × 0.5	0.76	47	11.7
[21]	61.5	$(10.25)^2\pi$	0.51 × 0.51	1.7	42.7	15.4
[22]	12.4	$(4.6)^2\pi$	0.54 × 0.54	0.62	46.5	16.8
[23]	30	15.6 × 15.6	0.25 × 0.25	3.3	38.6	21.5
this work	11	$(3.47)^2\pi$	0.33 × 0.33	2.1	85.6	22.6

would have a phase distribution over the aperture that is near to the ideal state, thus providing a measured high efficiency of 85.6% and a large −1 dB gain bandwidth of 22.6%. Since the antenna structure is fully symmetric, dual polarisation based on the feed orientation can be obtained.

6 References

[1] Abdelrahman, A.H., Yang, F., Elsherbeni, A.Z., *et al.*: '*Analysis and design of transmitarray antennas*' (Morgan & Claypool, Williston, VT, USA, 2017)

[2] Datthanasombat, S., Amaro, L.R., Harrell, J.A., *et al.*: 'Layered lens antenna'. IEEE Antennas and Propagation Society Int. Symp., Boston, July 2001, pp. 777–780

[3] Abdelrahman, A.H., Yang, F., Elsherbeni, A.Z.: 'Transmission phase limit of multilayer frequency selective surfaces for transmitarray designs', *IEEE Trans. Antennas Propag.*, 2014, **62**, (2), pp. 690–697

[4] Rahmati, B., Hassani, H.R.: 'Low profile wideband slot transmitarray antenna', *IEEE Trans. Antenna Propag.*, 2015, **63**, (11), pp. 174–181

[5] Rahmati, B., Hassani, H.R.: 'High-efficient wideband slot transmitarray antenna', *IEEE Trans. Antenna Propag.*, 2015, **63**, (11), pp. 5149–5155

[6] Bagheri, M.O., Hassani, H.R., Rahmati, B.: 'Dual-band, dual-polarised metallic slot transmitarray antenna', *IET Microw. Antennas Propag.*, 2017, **11**, (3), pp. 402–409

[7] Tuloti, S.H.R., Rezaei, P., Hamedani, F.T.: 'High-efficient wideband transmitarray antenna', *IEEE Antennas Wirel. Propag. Lett.*, 2018, **17**, (5), pp. 817–820

[8] Pozar, D.M.: 'Flat lens antenna concept using aperture coupled microstrip patches', *Electron. Lett.*, 1996, **32**, (23), pp. 2109–2111

[9] Clemente, A., Dussopt, L., Sauleau, R., *et al.*: 'Wideband 400-element electronically reconfigurable transmitarray in X-band', *IEEE Trans. Antennas Propag.*, 2013, **61**, (10), pp. 5017–5027

[10] Kamada, S., Michishita, N., Yamada, Y.: 'Metamaterial lens antenna using dielectric resonators for wide angle beam scanning'. IEEE Antennas and Propagation Society Int. Symp. APS-URSI, Toronto, Canada, July 2010

[11] Li, M., Behdad, N.: 'Ultra-wideband, true-time-delay, metamaterial-based microwave lenses'. IEEE Antennas and Propagation Society Int. Symp. APS-URSI, Chicago, IL, July 2012

[12] Zainud-Deen, S.H., Gaber, S.M., Awadalla, K.H.: 'Transmitarray using perforated dielectric material for wideband applications', *Prog. Electromagn. Res.*, 2012, **24**, pp. 1–13

[13] Al-Nuaimi, M.K.M., Hong, W.: 'Discrete dielectric reflectarray and lens for E-band with different feed', *IEEE Antennas Wirel. Propag. Lett.*, 2014, **13**, (12), pp. 947–950

[14] Mahmoud, A.-E., Hong, W., Zhang, Y., *et al.*: 'W-band multilayer perforated dielectric substrate lens', *IEEE Antennas Wirel. Propag. Lett.*, 2014, **13**, pp. 734–737

[15] Yi, H., Qu, S.W., Ng, K.B., *et al.*: '3-D printed millimetre wave and terahertz lenses with fixed and frequency scanned beam', *IEEE Trans. Antennas Propag.*, 2016, **64**, (2), pp. 442–449

[16] Wuang, M., Xu, S., Yang, F., *et al.*: 'Design of a Ku-band triple layer perforated dielectric transmitarray antenna'. IEEE Int. Symp. on Antennas and Propagation and URSI/USNC National Radio Science Meeting, Fajardo, Puerto Rico, 2016

[17] Wu, K.: '*Slow wave structures*' (John Wiley & Sons, Inc., 2005)

[18] Kock, W.E.: 'Metal-lens antennas', *Proc. IRE*, 1946, **34**, pp. 828–836

[19] Ryan, C.G.M., Chaharmir, M.R., Shaker, J., *et al.*: 'A wideband transmitarray using dual-resonant double square rings', *IEEE Trans. Antennas Propag.*, 2010, **58**, (5), pp. 1486–1493

[20] Abdelrahman, A.H., Nayeri, P., Esherbeni, A.Z., *et al.*: 'Bandwidth improvement methods of transmitarray antenna', *IEEE Trans. Antennas Propag.*, 2015, **63**, (7), pp. 2946–2954

[21] Jouanlanne, C., Clemente, A., Huchard, M., *et al.*: 'Wideband linearly polarized transmitarray antenna for 60 GHz backhauling', *IEEE Trans. Antennas Propag.*, 2017, **65**, (3), pp. 1440–1445

[22] Tian, C., Jiao, Y.-C., Zhao, G., *et al.*: 'A wideband transmitarray using triple-layer elements combined with cross slots and double square rings', *IEEE Antennas Wirel. Propag. Lett.*, 2017, **16**, pp. 1561–1564

[23] Massaccesi, A., Pirinoli, P., Bertana, V., *et al.*: '3D-printable dielectric transmitarray with enhanced bandwidth at millimeter-waves', *IEEE. Access*, 2018, **6**, pp. 46407–46418